Dalton Transactions

Accepted Manuscript

ROYAL SOCIETY OF CHEMISTRY

www.rsc.org/dalton

Gas-Phase Reaction of $CeVO_5^+$ Cluster Ions with C_2H_4: Reactivity of Cluster Bonded Peroxides

Jia-Bi Ma,*[a] Jing-Heng Meng[b] and Sheng-Gui He*[b]

[a] Dr. J.-B. Ma
Key Laboratory of Cluster Science, The Institute for Chemical Physics, School of Chemistry
Beijing Institute of Technology, 100081, Beijing (People's Republic of China)
E-Mail: majiabi@bit.edu.cn

[b] J.-H. Meng and Prof. Dr. S.-G. He
State Key Laboratory for Structural Chemistry of Unstable and Stable Species
Institute of Chemistry, Chinese Academy of Sciences
100190 Beijing (People's Republic of China)
E-Mail: shengguihe@iccas.ac.cn

Abstract

Cerium-vanadium oxide cluster cations $CeVO_5^+$ were generated by laser ablation, mass-selected by a quadrupole mass filter, thermalized through collisions with helium atoms, and then reacted with ethene molecules in a linear ion trap reactor. The cluster reactions have been characterized by time-of-flight mass spectrometry and density functional theory calculations. The $CeVO_5^+$ cluster has a closed-shell electronic structure and contains a peroxide (O_2^{2-}) unit. The cluster bonded O_2^{2-} species is reactive enough to oxidize a C_2H_4 molecule to generate $C_2H_4O_2$ that can be an acetic acid molecule. Atomic oxygen radicals ($O^{-\bullet}$), super-oxide radicals ($O_2^{-\bullet}$), and peroxides are three common reactive oxygen species. The reactivity of cluster bonded $O^{-\bullet}$ and $O_2^{-\bullet}$ radicals have been widely studied while the O_2^{2-} species were generally thought to be much less reactive or inert toward small molecules under thermal collision conditions. This work is among the first to report reactivity of peroxide unit on transition metal oxide clusters with hydrocarbon molecules, to the best of our knowledge.

Introduction

Recently, enormous interests in the research area of catalysis have been focused on determining the nature of active sites and reaction mechanisms in order to improve catalytic performance of a type of widely used catalysts, transition metal oxides (TMOs). The catalytic role of oxide surfaces is in terms of forming and providing oxygen in activated states.[1-8] In the scheme of O_2 dissociation: O_2 (molecular oxygen) $\rightarrow$ $O_2^{-\bullet}$ (superoxide radical) $\rightarrow$ O_2^{2-} (peroxide) $\rightarrow$ $2O^{-\bullet}$ (atomic oxygen radical) $\rightarrow$ $2O^{2-}$ (lattice oxygen), the $O_2^{-\bullet}$, O_2^{2-}, and $O^{-\bullet}$ are considered as reactive oxygen species (ROSs),[1,9,10] which have been proposed to play important roles in many practical reactions. For instance, transition metal peroxo complexes have been applied as catalysts in the epoxidation of olefins, aromatic oxidation, and in other reactions of industrial relevance.[11,12] However, obscured by low concentrations and very short lifetimes of the ROSs, as well as poorly understood aggregation and other effects, structure-property relationship of active sites involved with the ROSs is ill-defined for condensed phase systems.

Studies of gas-phase TMO clusters under isolated, well controlled, and well reproducible conditions provide an alternative way to understand the nature of active sites and the elementary steps involved in the ROS over the TMO catalysts. Recently, a value called oxygen-deficiency (Δ) has been defined for $M_xO_y^q$ oxide clusters:[13]

$$\Delta \equiv 2y - nx + q \qquad (1)$$

in which n is the highest oxidation state of M, and q is the charge number. A large body of investigations on the reactivity of TMO clusters indicated that the systems with unit oxygen-deficiency (Δ = 1) usually contain the $O^{-\bullet}$ radicals,[14-18] which can activate very stable molecules, such as CH_4 and CO, even at room temperature.[19-27] For clusters with larger Δ values (Δ > 1), the systems tend to form oxygen-oxygen bonds, that is superoxide or peroxide units. These superoxo and peroxo bonded clusters are usually less oxidative than the corresponding Δ = 1 clusters.[28] For instance, the lowest energy isomer of oxygen-rich cluster ScO_3^- contains a peroxo unit, which is inert toward *n*-butane, but its energetically competitive isomer with the $O^{-\bullet}$ radicals can activate *n*-C_4H_{10}.[29] In addition, some clusters containing $O_2^{-\bullet}$ are reactive toward small molecules. It has been reported that $(ZrO_2)_{1-3}O^+$ (Δ = 3) clusters possess superoxide moieties and are oxidative toward alkenes and C_2H_2, which were investigated through guided-ion-beam mass spectrometry and density functional theory (DFT) calculations.[30] It is noteworthy that $O^{-\bullet}$ and $O_2^{-\bullet}$

bonded TMO clusters are typical open-shell species. In contrast, the O_2^{2-} bonded TMO clusters are usually closed-shell systems of which the reactivity with small molecules such as hydrocarbons under thermal collision conditions has not been reported, to the best of our knowledge.

In the past few years, the study of heteronuclear oxide clusters has been reported to serve as a more detailed molecular approach for the understanding of the active sites of multi-component catalysts.[31-51] Heteronuclear oxide clusters exhibit features differing from their homonuclear counterparts in gas-phase reactions, such as in the reactions with CH_4.[52] Among the reported heteronuclear oxide clusters, the $Ce_xV_yO_z^+$ were investigated through infrared spectroscopy[39] as well as mass spectrometry[51] in conjunction with DFT calculations. The Ce^{+3}/V^{+5} rather than Ce^{+4}/V^{+4} was predicted to be favored in $Ce_xV_yO_z^+$ clusters.[39,51] The $CeV_2O_7^+$ cluster has been reported as the first bimetallic oxide cluster ion which gives rise to C=C bond cleavage of ethene.[51] The reactivity of atomic clusters varies dramatically with respect to their compositions, and it is worthy to investigate other oxygen-rich ($\Delta > 1$) $Ce_xV_yO_z^+$ clusters which may display intriguing reaction channels with small molecules, such as C_2H_4.

In this context, the electronic structure and reactivity of heteronuclear oxide cluster cations $CeVO_5^+$ ($\Delta = 2$) were studied by using mass spectrometry and DFT calculations. An interesting finding is that the $CeVO_5^+$ cluster with a peroxide unit O_2^{2-} and a closed-shell electronic structure can oxidize a C_2H_4 molecule to generate $C_2H_4O_2$ that can be an acetic acid molecule.

Methods

Experimental details

The details of the experimental setup can be found in the previous studies,[53] and only a brief outline of the experiments is given below. The cerium-vanadium oxide clusters were generated by pulsed laser ablation of a rotating and translating metal disk in the presence of about 1 % O_2 seeded in a He carrier gas (99.999%) with a backing pressure of 5 atm. The disk was a mixed cerium and vanadium powder with the molar ratio of 1:10. A 532 nm (second harmonic of Nd^{3+}:yttrium aluminum garnet-YAG) laser with an energy of 5-8 mJ /pulse and a repetition rate of 10 Hz was used. The carrier gas was controlled by a pulsed valve (General Valve, Series 9). In order to eliminate the water impurity that often occurs in the cluster distribution, the prepared gas mixture (O_2/He) was passed through a 10 m long copper tube coil at low temperature (T = 77 K)

before entering into the pulsed valve. The clusters of interest ($CeVO_5^+$) were mass-selected by a quadrupole mass filter (QMF) and enter into a linear ion trap (LIT) reactor, where they were thermalized by collisions with a pulse of He gas and then interacted with a pulse of C_2H_4 for a period of time. The assessment of thermalization for the cluster ions in the LIT reactor can be found in the previous studies.[53,54] The cluster ions ejected from the LIT were detected by a reflectron time-of-flight mass spectrometer (TOF-MS).[55] Assuming a pseudo-first order reaction mechanism, the ion intensities of clusters in reactions can be calculated and least-square fitted to the experimental data to determine the experimental rate constants (k_1).[56]

Theoretical details

All DFT calculations were performed with the Gaussian09[57] program package employing the hybrid B3LYP exchange-correlation functional[58-60]. The TZVP basis sets[61] were selected for V, C, O, H atoms, and D95 V basis set combined with Stuttgart/Dresden relativistic effective core potential[62] (denoted as SDD in Gaussian 09) was selected for Ce atom. Although the same functional and basis sets had been adopted for many reaction systems involving vanadium oxide and cerium oxide clusters in the literatures,[14,15,17,63-68] various functionals were still tested by calculating the bond dissociation energies of Ce–O, V–O, O–O, and C–H, and comparing with available experimental data (Table S1 in Supporting Information). It turned out that with the above basis sets, B3LYP functional is the overall best. A Fortran code based on genetic algorithm was used to generate initial guess structures of the cluster.[69] The coupled-cluster method with single, double, and perturbative triple excitations method CCSD(T)[70,71] with the above basis sets was used to calculate the single-point energies at the B3LYP optimized structures. Geometry optimizations of all reaction intermediates and TSs on the potential energy surfaces (PESs) were performed with full relaxation of all atoms. Vibrational frequency calculations are performed to check that the reaction intermediates and transition state (TS) species had zero and one imaginary frequency, respectively. Intrinsic reaction-coordinate (IRC) calculations[72-76] were also performed to connect the TS with local minima. The zero-point vibration corrected energies (ΔH_{0K}) are reported in this work. Both singlet and triplet spin states were tested for the intermediates and TSs, and in most cases the singlets were found to be more stable than the triplets.

Results and Discussion

Cerium has four stable isotopes: ^{136}Ce (0.19%), ^{138}Ce (0.25%), ^{140}Ce (88.45%), and ^{142}Ce (11.11%) of which the former two have negligible abundances. The TOF mass spectrum for laser-ablation-generated and mass-selected $^{140}CeVO_5^+$ cluster ions (m/z = 271) is shown in Fig. 1a. The mass resolution of the QMF used in the experiments was good enough to select $^{140}CeVO_5^+$ from $^{142}CeVO_5^+$ while a mass peak (m/z = 257) corresponding the mass loss of 14 amu with respect to $^{140}CeVO_5^+$ was always present in the spectrum. This peak is assigned as $^{140}CeVO_3H_2O^+$ that can be generated from the reaction of $^{140}CeVO_5^+$ with water impurity during the process of confining and cooling the $^{140}CeVO_5^+$ cluster ions in the LIT:

$$CeVO_5^+ + H_2O \rightarrow CeVO_3H_2O^+ + O_2 \quad (2)$$

The above substitution reaction indicates that there can be an O–O unit in the $CeVO_5^+$ cluster. When Ar atoms were delivered to the LIT reactor as reactant gas, no additional product such as $CeVO_3^+$ that could be produced from collision induced dissociation (CID, $CeVO_5^+ + Ar \rightarrow CeVO_3^+ + O_2 + Ar$) was generated as can be seen from Fig. 1b. This suggests that the O–O unit in $CeVO_5^+$ is quite strongly bonded.

Upon the reactions with 0.05 Pa C_2H_4 for about 1.1 ms as shown in Fig. 1c, new products $CeVO_3^+$ and $CeVO_5C_2H_4^+$, which are not present in the interaction of $CeVO_5^+$ with Ar (Fig. 1b), were generated. The relative intensities of these two products increase as the C_2H_4 pressure increases (Fig. 1d), which suggests the following reaction channels:

$$CeVO_5^+ + C_2H_4 \rightarrow CeVO_5C_2H_4^+ \quad (3a)$$

$$CeVO_5^+ + C_2H_4 \rightarrow CeVO_3^+ + C_2H_4O_2 \quad (3b)$$

It is noteworthy that $CeVO_3^+$ is absent in Fig. 1b, so this product cluster observed in Figs. 1c and 1d is indeed from chemical reaction (the above channel 3b) rather than from the CID with C_2H_4. Fig. 1d indicates that additional weak product peaks that can be assigned as $CeVO_4^+$ and $CeVO_5(C_2H_4)_2^+$ were also generated when relatively high pressure of C_2H_4 in the reactor was used.

(Fig. 1 near here, please)

Fig. 2 shows the signal variation of the reactant and product cluster ions in $CeVO_5^+ + C_2H_4$ with respect to the reactant gas pressure in the reactor. The relative ion intensities of reactants and products can be well fitted by assuming a pseudo-first-order reaction mechanism. Although the

formation of molecule association product $CeVO_5C_2H_4^+$ is a major reaction channel, the signal increase of $CeVO_3^+$ is still apparent with the increase of the reactant gas pressure. The relative ion intensity of $CeVO_3H_2O^+$ does not change within the experimental uncertainties, suggesting that it was generated during confining and cooling the $CeVO_5^+$ cluster ions. The pseudo-first-order rate constant (k_1) of the overall reaction was determined to be $k_1(CeVO_5^+ + C_2H_4) = 5.4 \times 10^{-11}$ cm^3 s^{-1} molecule^{-1}, corresponding to an efficiency (ø) of 6%.[77] In the reaction of $CeVO_5^+$ with C_2H_4, the double oxygen atom transfer (DOAT) process, reaction channel 3b, is very interesting. This process has a branching ratio of 16%.

(Fig. 2 near here, please)

The DFT calculated structures of $CeVO_5^+$ are shown in Fig. 3. The lowest energy isomer of $CeVO_5^+$ predicted by B3LYP (IS1) contains an side-on peroxo unit (η^2-O_2^{2-}) with O–O bond length of 143 pm. In other energetically low lying isomers of $CeVO_5^+$, O_2^{2-} units generally exist as bridging peroxide unit (IS2 and IS3), and in μ-η^2:η^2 (IS4 and IS11), μ-η^2:η^1 (IS10), or η^2 (IS5 and the rest of isomers) fashions. The existence of the O_2^{2-} unit in the cluster is generally consistent with the observation of the substitution reaction (2) by the experiment.

Considering that the relative energies of isomers IS1-IS5 are close, single point CCSD(T) calculations were performed for IS1-IS5. The relative energies of these isomers by CCSD(T) are slightly different from those by B3LYP. The relative energy difference is around 0.1-0.2 eV, which indicates that the precision of B3LYP calculations on relative energies may not be better than 0.2 eV. Because IS1-IS5 are close in energy in both B3LYP and CCSD(T) calculations, all of them are the candidates of the ground state structure of $CeVO_5^+$. It should be pointed out that with respect to the identification of the lowest-energy structure of clusters, spectroscopic methods, such as infrared vibrational predissociation spectroscopy, would be helpful. The infrared spectra of IS1-IS5 are given in Fig. S1 of the Supporting Information. The vibrational frequencies may be used for future experimental identification of these clusters.

(Fig. 3 near here, please)

The reaction pathways of the five isomers IS1-IS5 with C_2H_4 were all followed by the DFT

calculations. Among these pathways, the one for reaction of IS4 with C_2H_4 involves the lowest TS, which renders it the most possible structure for $CeVO_5^+$. In IS4, the peroxide unit with O–O bond length of 141 pm is bonded with both cerium and vanadium atoms. As shown in Fig. 4, this path commences with the generation of the encounter complex **1**, and then epoxyethane unit is formed in **2** via **TS1/2** that is only 0.05 eV higher in energy compared to the entrance channel. Note that this small energy barrier can be surmountable by the cluster vibrational energy (0.29 eV at T = 298 K by DFT) and the center-of-mass collisional energy (around 0.04 eV) between $CeVO_5^+$ and C_2H_4. The activation of the peroxo unit is also achieved in the sequence **1** → **TS1/2** → **2**, resulting in the formation of $O_tCe(O_b)_2V(O_t)_2$ moiety (O_b and O_t are bridging and terminal oxygen atoms, respectively) and a large energy release. From **2**, the reaction pathway bifurcates and two different products form. The newly formed epoxyethane unit can be directly released, leading to the formation of epoxyethane (C_2H_4O) and $CeVO_4^+$ (**8**). The structure of $CeVO_4^+$ cluster shown here is in line with that reported in Ref. 39. It is noteworthy that the $CeVO_4^+$ product was indeed generated in the experiment although the signal was very weak (Fig. 1d). The other pathway is the DOAT, which brings about formation of $CeVO_3^+$ (**7**) and $C_2H_4O_2$. There are several reasonable structures for $C_2H_4O_2$, in which acetic acid (denoted as HAc) is the thermochemically most favored products. Sufficient energy (-4.50 eV with respect to the reactants) is gained in the step of **2** → **TS2/3** → **3**, which can be used to surmount the following large reaction barrier **TS3/4**. It can be seen that intramolecular hydrogen atom transfer (HAT) process is a rather energy demanding step. The generated HAT-intermediate **4** contains a newly formed hydroxyl group, and the migration of the second hydrogen atom takes place via **4** → **TS4/5** → **5**, which is kinetically less energy demanding than the first HAT step (**3** → **TS3/4** → **4**). From **5**, the O_t atom bound to vanadium atom is transferred from $CeVO_4$ moiety to the less coordinated carbon atom of CH_3COH unit, thus generating a HAc group in **6**. According to a relax scan of V–O bond in **6**, the HAc group is liberated without the involvement of any further intermediates or transition structures, and the DOAT process completes. Notably, for the intermediate **6** and the product **7**, the triplet states are lower in energy than the corresponding singlet states, and the spin conversion[78] from singlet to triplet may take place in the step of **5** ⟶ **TS5/6** ⟶ **6**. The details of spin conversion are not considered herein because of little relevance to the conclusions. In addition, IRC calculations for the key steps of **1** → **TS1/2** → **2**, and **3** → **TS3/4** → **4** are shown in Fig. S2 of the Supporting Information, to

illustrate how these barriers connect local minima.

(Fig. 4 near here, please)

Notably, starting from intermediate **2**, the generation of $CeVO_3^+$ (**7**) + HAc is kinetically less competitive than that of $CeVO_4^+$ (**8**) + C_2H_4O, due to the existence of a relatively higher energy of **TS3/4** (-1.30 eV) than that of **8** + C_2H_4O (-1.59 eV). The DFT calculations suggest that single oxygen atom transfer (**8**/C_2H_4O) may correspond to the main reaction channel in comparison with DOAT (**7**/HAc), which is not totally in line with the experimental results. However, these two pathways predicted by DFT calculations are favorable thermodynamically and kinetically, indicating that both of them could take place and be observable under the experimental conditions. Thus, although the DFT results do not predict the correct branching ratios of generating $CeVO_4^+$ and $CeVO_3^+$, the calculations of $CeVO_5^+$ + C_2H_4 generally support the experiments.

Other reaction pathways have also been carefully investigated. For the PES of IS1 with C_2H_4, breaking the O–O bond of peroxide unit is a quite energy demanding step, as shown in Fig. S3 in the Supporting Information, and the highest reaction barrier (**TS2/3'**) is 0.28 eV higher in energy with respect to the separated reactants, via which the activation of O_2^{2-} completes. As **TS2/3'** is located above the entrance energy of reactants, this thermochemically rather favored step is kinetically impeded. In the reaction pathways starting from IS2 and IS3 with C_2H_4 (Figs. S4 and S5 in the Supporting Information, respectively), the first oxygen-atom transfer results in the formation of formaldehyde (CH_3CHO); it is not accessible to transfer a second oxygen atom to the loosely bound CH_3CHO units, which can evaporate easily from the reaction complex. The paths originating from other intermediates (Figs. S6 and S7 in the Supporting Information) and alternative oxygen sites of IS1, IS2 and IS3 (Fig. S8) as well as the reaction of IS5 with C_2H_4 (Fig. S9, Supporting Information) have also been tested, while relatively large barriers are inevitably involved, indicating that these pathways are kinetically impeded. The obtained results suggest that hydrogen-atom transfer is an energy-demanding step, and only a relatively high energy gain can overcome such a barrier.

Among the five isomers of $CeVO_5^+$ cluster, IS1-IS5 shown in Fig. 3, the bonding character of peroxide unit in IS4 is quite special, and O_2^{2-} unit is bonded with both cerium and vanadium atoms.

In contrast, the η^2-O_2^{2-} unit bound to either V atom (IS1) or Ce atom (IS5) is much less reactive with C_2H_4 as can be seen from the investigated reaction pathways. Although O–O bond lengths of peroxide units in IS1 and IS4 are similar (143 and 141 pm, respectively), in the reaction with C_2H_4, it is much easier to activate the O_2^{2-} unit in IS4 than in IS1. The results indicate that the reactivity of the peroxide units in homonuclear vanadium or cerium oxide clusters may be sluggish, which is in line with the fact that no O_2^{2-} bonded vanadium or cerium oxide cluster has been reported to be reactive toward ethane under thermal collision conditions. In the gas-phase studies, the importance of doping effect in heteronuclear oxide clusters[31-51] has been identified. Changing the compositions of cluster systems can affect the distributions of local charge[38] and spin density[63], as well as reaction mechanisms,[41] leading to distinguishing features of heteronuclear oxide clusters. The results also suggest the intriguing role of doping effect on chemical reactions in general.

It is noteworthy that the DOAT channel usually happens in open-shell cluster systems with unsaturated hydrocarbon, such as C_2H_4 or C_2H_2. For instance, this channel has been reported in the reactions of $(CeO_2)_n^+$ (n = 2-6) with C_2H_2,[64] $V_4O_{10}^+$ with $C_2H_{2,4}$,[79] and $CeV_2O_7^+$ with C_2H_4[51]; while all of these reactive clusters contain the $O^{-\bullet}$ radicals and are open-shell species. However, the $CeVO_5^+$ cluster in this study has a closed-shell electronic structure, and DOAT was observed the reaction with C_2H_4.

Conclusions

The gas-phase reaction of oxygen-rich cluster $CeVO_5^+$ toward C_2H_4 has been investigated using a reflectron time-of-flight mass spectrometry coupled with a laser ablation cluster source, a quadrupole mass filter, and a linear ion trap reactor. Reaction channels for generation of $CeVO_3^+/C_2H_4O_2$ and $CeVO_5C_2H_4^+$ have been identified. The DFT calculations indicated that the $CeVO_5^+$ has closed-shell electronic structure and contain a peroxide unit, which is reactive enough to oxidize a C_2H_4 molecule to generate acetic acid. To the best of our knowledge, this work is among the first to identify the reactivity of peroxide unit with hydrocarbon molecules on TMO clusters with closed-shell electronic structures, which shed light on the molecular view of the reactivity of peroxo complexes in related condensed-phase systems. This study also emphasizes that in gas-phase studies, the reactions of heteronuclear oxide clusters with small molecules can

exhibit very different features compared with those of homonuclear oxide clusters.

Acknowledgements

This work was supported by Beijing Natural Science Foundation (Grant No. 2144055), the Basic Research Fund of Beijing Institute of Technology (Grant No. 20121942012), and the Natural Science Foundation of China (Grant No. 21325314). We thank Prof. X.-L. Ding and Zhen Yuan for insightful disccussions.

References

1. M. Che and A. J. Tench, *Adv. Catal.* 1982, **31**, 77.
2. M. Che and A. J. Tench, *Adv. Catal.* 1983, **32**, 1.
3. H. J. Freund, *Chem. Eur. J.* 2010, **16**, 9384.
4. M. Chiesa, E. Giamello and M. Che, *Chem. Rev.* 2010, **110**, 1320.
5. M. V. Ganduglia-Pirovano, C. Popa, J. Sauer, H. Abbott, A. Uhl, M. Baron, D. Stacchiola, O. Bondarchuk, S. Shaikhutdinov and H. J. Freund, *J. Am. Chem. Soc.* 2010, **132**, 2345.
6. H. Kuhlenbeck, S. Shaikhutdinov and H. J. Freund, *Chem. Rev.* 2013, **113**, 3986.
7. H. J. Freund, *Catal. Today* 2014, **238**, 2.
8. T. Kropp, J. Paier and J. Sauer, *J. Am. Chem. Soc.* 2014, **136**, 14616, and references herein.
9. G. I. Panov, K. A. Dubkov and E. V. Starokon, *Catal. Today* 2006, **117**, 148.
10. L. Can, K. Domen, K. Maruya and T. Onishi, *J. Am. Chem. Soc.* 1989, **111**, 7683.
11. W. A. Herrmann, J. D. G. Correia, F. E. Kuhn, G. R. J. Artus and C. C. Romao, *Chem. Eur. J.* 1996, **2**, 168.
12. D. V. Deubel, J. Sundermeyer and G. Frenking, *Inorg. Chem.* 2000, **39**, 2314.
13. Y.-X. Zhao, X.-L. Ding, Y.-P. Ma, Z.-C. Wang and S.-G. He, *Theor. Chem. Acc.* 2010, **127**, 449.
14. D. R. Justes, R. Mitrić, N. A. Moore, V. Bonačić-Koutecký and A. W. Castleman Jr, *J. Am. Chem. Soc.* 2003, **125**, 6289.
15. F. Dong, S. Heinbuch, Y. Xie, E. R. Bernstein, J. J. Rocca, Z. C. Wang, X. L. Ding and S. G. He, *J. Am. Chem. Soc.* 2009, **131**, 1057.
16. G. E. Johnson, R. Mitrić, M. Nossler, E. C. Tyo, V. Bonačić-Koutecký and A. W. Castleman., *J. Am. Chem. Soc.* 2009, **131**, 5460.
17. X.-N. Wu, X.-L. Ding, S.-M. Bai, B. Xu, S.-G. He and Q. Shi, *J. Phys. Chem. C* 2011, **115**, 13329.
18. X.-N. Wu, S.-Y. Tang, H.-T. Zhao, T. Weiske, M. Schlangen and H. Schwarz, *chemistry – A European Journal* 2014, **20**, 6672
19. D. K. Böhme and H. Schwarz, *Angew. Chem., Int. Ed.* 2005, **44**, 2336.
20. G. E. Johnson, R. Mitrić, V. Bonačić-Koutecký and A. W. Castleman Jr, *Chem. Phys. Lett.* 2009, **475**, 1.
21. J. Roithová and D. Schröder, *Chem. Rev.* 2010, **110**, 1170.
22. H. Schwarz, *Angew. Chem., Int. Ed.* 2011, **50**, 10096.
23. Y.-X. Zhao, X.-N. Wu, J.-B. Ma, S.-G. He and X.-L. Ding, *Phys. Chem. Chem. Phys.* 2011, **13**, 1925.
24. X.-L. Ding, X.-N. Wu, Y.-X. Zhao and S.-G. He, *Acc. Chem. Res.* 2012, **45(3)**, 382.
25. N. Dietl, M. Schlangen and H. Schwarz, *Angew. Chem. Int. Ed.* 2012, **51**, 5544.
26. S. Yin and E. R. Bernstein, *Int. J. Mass Spectrom.* 2012, **321-322**, 49.
27. Q.-Y. Liu and S.-G. He, *Chem. J. Chinese U.* 2014, **35**, 665.
28. Z.-C. Wang, X.-L. Ding, Y.-P. Ma, H. Cao, X.-N. Wu, Y.-X. Zhao and S.-G. He, *Chinese Sci. Bull.* 2009, **54**, 2814.
29. L.-H. Tian, Y.-X. Zhao, X.-N. Wu, X.-L. Ding, S.-G. He and T.-M. Ma, *ChemPhysChem* 2012, **13**, 1282.
30. E. C. Tyo, M. Nossler, C. L. Harmon, R. Mitrić, V. Bonačić-Koutecký and A. W. Castleman Jr, *J. Phys. Chem. C* 2011, **115**, 21559.
31. Z.-C. Wang, X.-N. Wu, Y.-X. Zhao, J.-B. Ma, X.-L. Ding and S.-G. He, *Chem. Phys. Lett.* 2010, **489**, 25.
32. J.-B. Ma, X.-N. Wu, Y.-X. Zhao, X.-L. Ding and S.-G. He, *Phys. Chem. Chem. Phys.* 2010, **12**, 12223
33. X.-L. Ding, Y.-X. Zhao, X.-N. Wu, Z.-C. Wang, J.-B. Ma and S.-G. He, *Chem. Eur. J.* 2010, **16**, 11463.
34. Y.-X. Zhao, X.-N. Wu, J.-B. Ma, S.-G. He and X.-L. Ding, *J. Phys. Chem. C* 2010, **114**, 12271.

35. N. Dietl, R. F. Höckendorf, M. Schlangen, M. Lerch, M. K. Beyer and H. Schwarz, *Angew. Chem., Int. Ed.* 2011, **50**, 1430.
36. Z.-C. Wang, N. Dietl, R. Kretschmer, T. Weiske, M. Schlangen and H. Schwarz, *Angew. Chem. Int. Ed.* 2011, **50**, 12351.
37. Z.-C. Wang, X.-N. Wu, Y.-X. Zhao, J.-B. Ma, X.-L. Ding and S.-G. He, *Chem. Eur. J.* 2011, **17**, 3449.
38. Z.-Y. Li, Y.-X. Zhao, X.-N. Wu, X.-L. Ding and S.-G. He, *Chem. Eur. J.* 2011, **17**, 11728.
39. L. Jiang, T. Wende, P. Claes, S. Bhattacharyya, M. Sierka, G. Meijer, P. Lievens, J. Sauer and K. R. Asmis, *J. Phys. Chem. A* 2011, **115**, 11187.
40. Z.-C. Wang, S. Yin and E. R. Bernstein, *J. Phys. Chem. Lett.* 2012, **3**, 2415.
41. J.-B. Ma, Z.-C. Wang, M. Schlangen, S.-G. He and H. Schwarz, *Angew. Chem. Int. Ed.* 2012, **51**, 5991.
42. X.-N. Li, X.-N. Wu, X.-L. Ding, B. Xu and S.-G. He, *Chem. Eur. J.* 2012, **18**, 10998.
43. N. Dietl, T. Wende, K. Chen, L. Jiang, M. Schlangen, X. Zhang, K. R. Asmis and H. Schwarz, *J. Am. Chem. Soc.* 2013, **135**, 3711
44. N. Dietl, X. H. Zhang, C. van der Linde, M. K. Beyer, M. Schlangen and H. Schwarz, *Chem. Eur. J.* 2013, **19**, 3017.
45. J.-B. Ma, Z.-C. Wang, M. Schlangen, S.-G. He and H. Schwarz, *Angew. Chem. Int. Ed.* 2013, **52**, 1226.
46. X.-N. Wu, X.-N. Li, X.-L. Ding and S.-G. He, *Angew. Chem. Int. Ed.* 2013, **52**, 2444
47. Z.-C. Wang, J.-W. Liu, M. Schlangen, T. Weiske, D. Schröder, J. Sauer and H. Schwarz, *Chem. Eur. J.* 2013, **19**, 11496.
48. Z.-C. Wang, S. Yin and E. R. Bernstein, *J. Chem. Phys.* 2013, **139**, 194313.
49. Z. Yuan, X.-N. Li and S.-G. He, *J. Phys. Chem. Lett.* 2014, **5**, 1585.
50. X.-N. Li, Z. Yuan and S.-G. He, *J. Am. Chem. Soc.* 2014, **136**, 3617.
51. J.-B. Ma, Z. Yuan, J.-H. Meng, Q.-Y. Liu and S.-G. He, *ChemPhysChem* 2014, DOI: 10.1002/cphc.201402347.
52. H. Schwarz, *Isr. J. Chem.* 2014, **54**, 1413.
53. Z. Yuan, Z.-Y. Li, Z.-X. Zhou, Q.-Y. Liu, Y.-X. Zhao and S.-G. He, *J. Phys. Chem. C* 2014, **118**, 14967.
54. Y.-X. Zhao, Z.-Y. Li, Z. Yuan, X.-N. Li and S.-G. He, *Angew. Chem. Int. Ed.* 2014.
55. X.-N. Wu, B. Xu, J.-H. Meng and S.-G. He, *Int. J. Mass Spectrom.* 2012, **310**, 57.
56. Z.-Y. Li, Z. Yuan, X.-N. Li, Y.-X. Zhao and S.-G. He, *J. Am. Chem. Soc.* 2014, **136**, 14307.
57. G. W. T. M.J. Frisch, H.B. Schlegel, G.E. Scuseria, M.A. Robb, J.R. Cheeseman, G. Scalmani, V. Barone, B. Mennucci, G. A. Petersson, H. Nakatsuji, M. Caricato, X. Li, H.P. Hratchian, A.F. Izmaylov, J. Bloino, G. Zheng, J.L. Sonnenberg, M. Hada, M. Ehara, K. Toyota, R. Fukuda, J. Hasegawa, M. Ishida, T. Nakajima, Y. Honda, O. Kitao, H. Nakai, T. Vreven, J.A. Montgomery, Jr., J.E. Peralta, F. Ogliaro, M. Bearpark, J.J. Heyd, E. Brothers, K.N. Kudin, V.N. Staroverov, R. Kobayashi, J. Normand, K. Raghavachari, A. Rendell, J.C. Burant, S.S. Iyengar, J. Tomasi, M. Cossi, N. Rega, J.M. Millam, M. Klene, J.E. Knox, J.B. Cross, V. Bakken, C. Adamo, J. Jaramillo, R. Gomperts, R.E. Stratmann, O. Yazyev, A.J. Austin, R. Cammi, C. Pomelli, J.W. Ochterski, R.L. Martin, K. Morokuma, V.G. Zakrzewski, G.A. Voth, P. Salvador, J.J. Dannenberg, S. Dapprich, A.D. Daniels, O. Farkas, J.B. Foresman, J.V. Ortiz, J. Cioslowski, D.J. Fox, Gaussian 09 Revision A.1, Gaussian Inc. Wallingford CT, 2009.
58. C. T. Lee, W. T. Yang and R. G. Parr, *Phys. Rev. B* 1988, **37**, 785.
59. A. D. Becke, *Phys. Rev. A* 1988, **38**, 3098.
60. A. D. Becke, *J. Chem. Phys.* 1993, **98**, 5648.
61. A. Schäfer, C. Huber and R. Ahlrichs, *J. Chem. Phys.* 1994, **100**, 5829.

62. D. Andrae, U. Häußermann, M. Dolg, H. Stoll and H. Preuß, *Theor. Chim. Acta.* 1990, **77**, 123.
63. X.-N. Wu, Y.-X. Zhao, W. Xue, Z.-C. Wang, S.-G. He and X.-L. Ding, *Phys. Chem. Chem. Phys.* 2010, **12**, 3984.
64. X.-L. Ding, X.-N. Wu, Y.-X. Zhao, J.-B. Ma and S.-G. He, *ChemPhysChem* 2011, **12**, 2110.
65. K. R. Asmis, T. Wende, M. Brummer, O. Gause, G. Santambrogio, E. C. Stanca-Kaposta, J. Dobler, A. Niedziela and J. Sauer, *Phys. Chem. Chem. Phys.* 2012, **14**, 9377.
66. J.-B. Ma, Y.-X. Zhao, S.-G. He and X.-L. Ding, *J. Phys. Chem. A* 2012, **116**, 2049.
67. S. Feyel, J. Dobler, D. Schröder, J. Sauer and H. Schwarz, *Angew. Chem., Int. Ed.* 2006, **45**, 4681.
68. B. L. Harris, T. Waters, G. N. Khairallah and R. A. J. O'Hair, *J. Phys. Chem. A* 2013, **117**, 1124.
69. X.-L. Ding, Z.-Y. Li, J.-H. Meng, Y.-X. Zhao and S.-G. He, *J. Chem. Phys.* 2012, **137**, 214311.
70. K. Raghavachari, G. W. Trucks, J. A. Pople and M. Headgordon, *Chem. Phys. Lett.* 1989, **157**, 479.
71. J. D. Watts, J. Gauss and R. J. Bartlett, *J. Chem. Phys.* 1993, **98**, 8718.
72. K. Fukui, *J. Phys. Chem.* 1970, **74**, 4161.
73. K. Fukui, *Acc. Chem. Res.* 1981, **14**, 363.
74. C. Gonzalez and H. B. Schlegel, *J. Chem. Phys.* 1989, **90**, 2154.
75. D. G. Truhlar and M. S. Gordon, *Science* 1990, **249**, 491.
76. C. Gonzalez and H. B. Schlegel, *J. Phys. Chem.* 1990, **94**, 5523.
77. G. Kummerlöwe and M. K. Beyer, *Int. J. Mass Spectrom.* 2005, **244**, 84.
78. D. Schröder, S. Shaik and H. Schwarz, *Acc. Chem. Res.* 2000, **33**, 139.
79. Z. Yuan, Y.-X. Zhao, X.-N. Li and S.-G. He, *Int. J. Mass Spectrom.* 2013, **354-355**, 105.

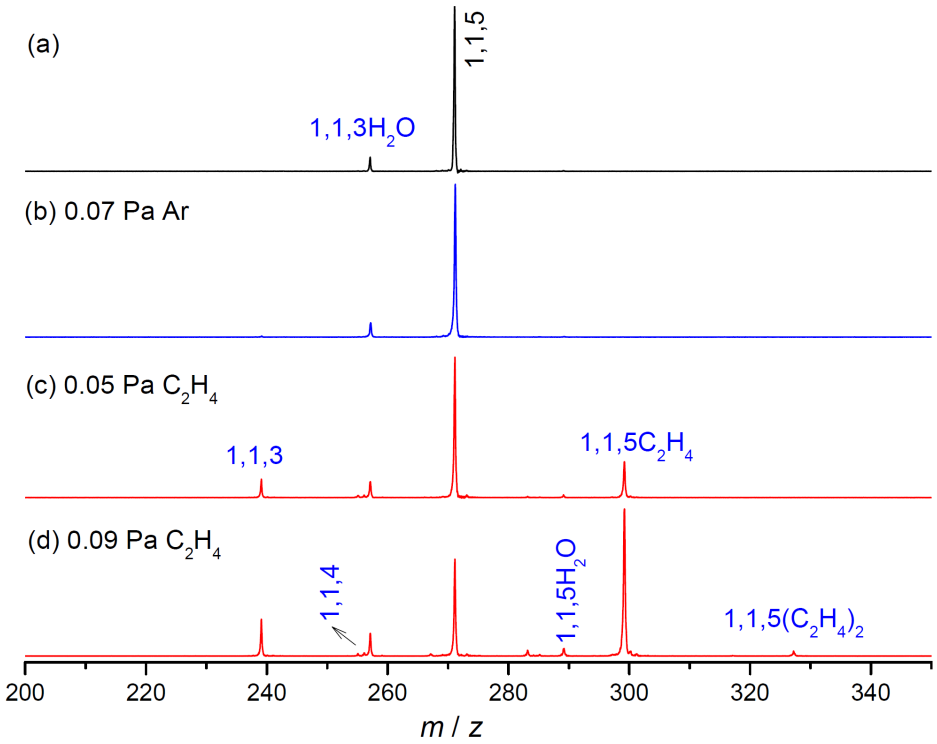

Figure 1. TOF mass spectra for the reactions of mass-selected $^{140}CeVO_5^+$ with Ar (b) and C_2H_4 (c,d) for 1.1 ms. The effective reactant gas pressures are shown.[53] The numbers *x*,*y*,*z*, and *x*,*y*,*z*X denote $Ce_xV_yO_z^+$ and $Ce_xV_yO_zX^+$ (X = C_2H_4, H_2O, etc.) clusters, respectively.

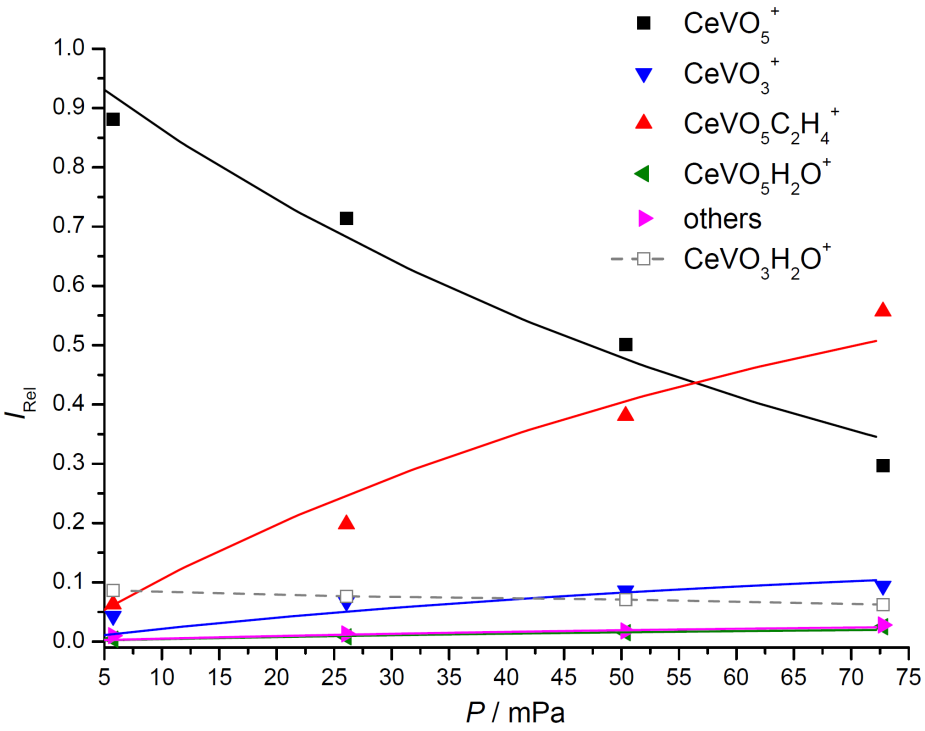

Figure 2. Variation of the relative intensities of the reactant and product cluster ions in the reaction between $CeVO_5^+$ and C_2H_4 with respect to the experimental reactant gas pressure. The solid lines are fitted to the experimental data points by using the equations derived with the approximation of the pseudo-first-order reaction mechanism.

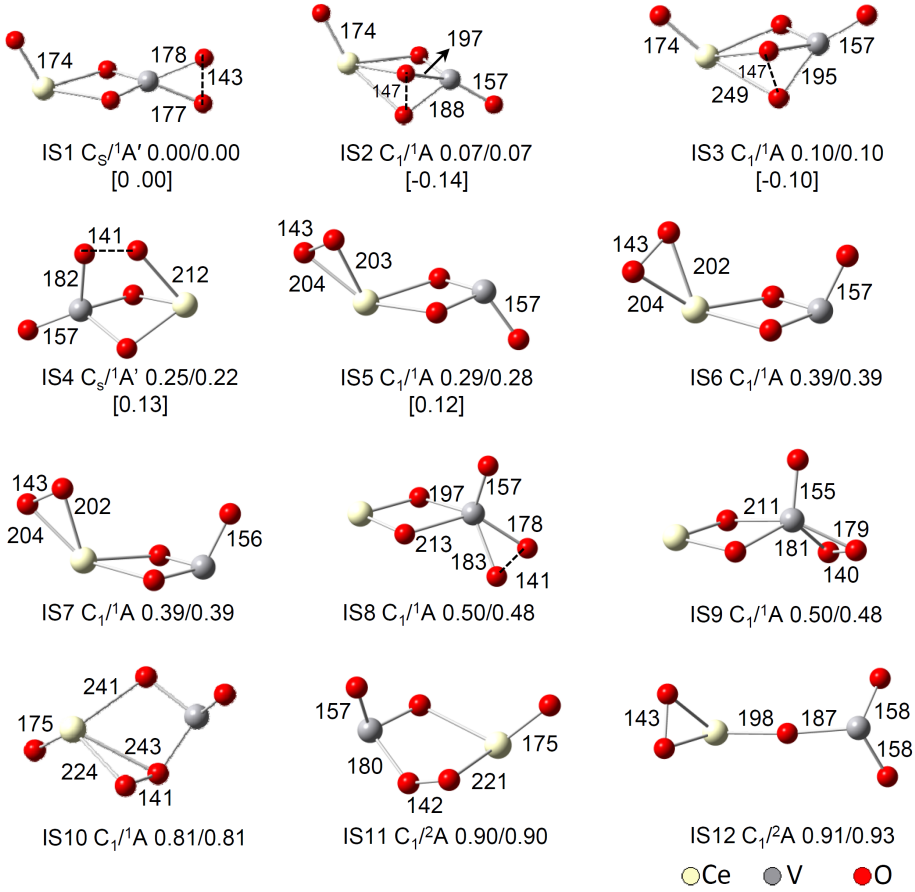

Figure 3. DFT calculated structures and relative energies of $CeVO_5^+$. The point group, electronic state, and energy (both with and without zero-point energy corrections, ΔE + ZPE/ΔE) in eV are given under each structure. Some bond lengths (in pm) are given. Relative energies by CCSD(T) are in square brackets.

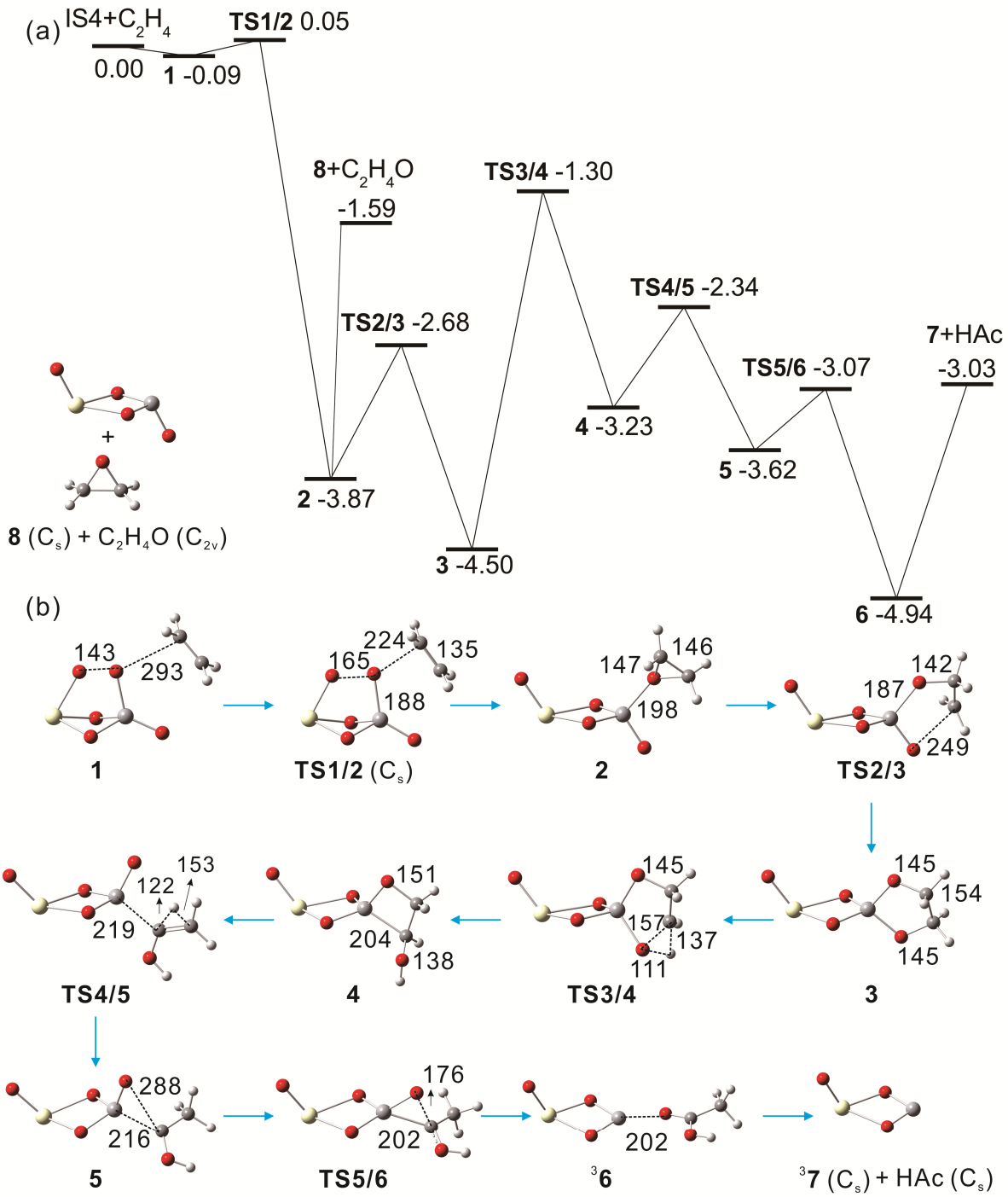

Figure 4. DFT calculated potential energy profiles (a) and structures (b) for reaction of IS4 with C_2H_4. In panel a, the zero-point vibration corrected energies (ΔH_{0K} in eV) of the reaction intermediates, transition states, and products with respect to the separated reactants are given. In panel b, bond lengths are in pm, and the superscripts indicate that the spin states of intermediate **6** and the product **7** are triplets. The symmetry is given below some structures in parentheses, and others with no parentheses have C_1 symmetry. Notably, the structures of **8** and C_2H_4O are given in the inset in panel a.

Table of Contents (TOC)

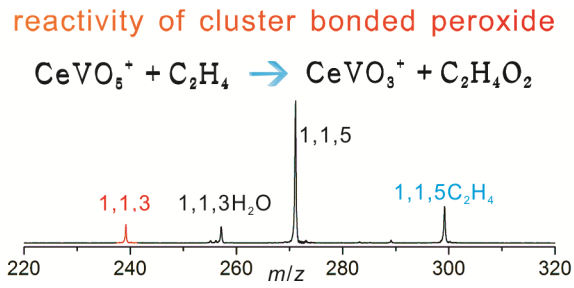

The reactivity of peroxide unit with hydrocarbon molecules on transition metal oxide cluster with closed-shell electronic structure has been first identified.